# Density Functional Theory Study of the Platinum-Catalyzed Cyclopropanation Reaction with Olefin

**Zhiyuan Geng,* Penji Yan, Yongcheng Wang, Xiaoqiang Yao, Yanxia Han, and Junxi Liang**

*Gansu Key Laboratory of Polymer Materials, College of Chemistry and Chemical Engineering Northwest Normal University, Lanzhou 730070, P.R. China*

*Received: April 26, 2007; In Final Form: July 2, 2007*

A computational study of the platinum-catalyzed cyclopropanation reaction with olefin is presented. The model system is formed by an ethylene molecule and the active catalytic species, which forms from a $CH_2$ fragment and the $Cl_2Pt(PH_3)_2$ complex. The results show that the active catalytic species is not a metal-carbene of the type $(PH_3)_2Cl_2Pt{=}CH_2$ but two carbenoid complexes which can exist in almost two degenerate forms, namely $(PH_3)_2Pt(CH_2Cl)Cl$ (carbenoid A) and $(PH_3)Pt(CH_2PH_3)Cl_2$ (carbenoid B). The reaction proceeds through three pathways: methylene transfer, carbometalation for carbenoid A, and the reaction of a monophosphinic species for carbenoids (A and B). The most favored reaction channel is methylene transfer pathway for $(PH_3)Pt(CH_2PH_3)Cl_2$ (carbenoid B) species with a barrier of 31.32 kcal/mol in gas phase. The effects of dichloromethane, THF, and benzene solvent are investigated with PCM method. For carbenoid A, both methylene transfer and carbometalation pathway barriers to reaction become remarkably lower with the increasing polarity of solvent (from 43.25 and 52.50 kcal/mol for no solvent to 25.36 and 38.53 kcal/mol in the presence of the dichloromethane). In contrast, the reaction barriers for carbenoid B via the methylene transfer path hoist 6.30 kcal/mol, whereas the barriers do not change significantly for the reaction path of a monophosphinic species for carbenoids (A and B).

## Introduction

Cyclopropane derivatives have been found in a wide range of natural and unnatural compounds that exhibit important biological activities and in an array of substances used as starting materials and intermediates in organic synthesis.[1−15] It has motivated a large number of research groups to develop new and wide-ranging methods to produce cyclopropanated products.[1−20] The cyclopropanation reaction catalyzed by transition metals has been known for many years and represents a very useful and well-documented process to synthesize cyclopropane rings.[2−4,15−34] To our best knowledge, many transition metals such as Rh, Ru, Pd, Pt, Ni, Cu, Zn, Sm, and Li are found to be able to catalyze cyclopropanation.[15−34] It is also generally accepted that transition metal-catalyzed cyclopropanation reactions proceed via a metal−carbene complex, which is formed by association of the diazo compound and the catalyst with concomitant extrusion of nitrogen. For example, copper-, ruthenium-, and osmium-carbene have previously been isolated from stoichiometric reactions with diazo esters and have proven to be an active catalyst in these processes.[15−18] However, other experimental results[28−35] suggest that the active species could be a carbenoid derivative similar to that proposed for the Simmons-Smith (SS)[35] reaction. Following, a great deal of work has been done to improve and develop alternative to produce SS-type reagents. For example, in 1995, McCrindle and coworkers[36] isolated α-halogenomethyl derivatives of palladium and platinum, and for the two complexes $(PPh_3)_2Pd(CH_2Cl)Cl$ and $(PPh_3)_2Pt(CH_2Cl)Cl$, they studied in detail the X-ray structures. However, compared with Zn, Sm, Rh, Ru, Ni, Pd, Cu, and Li,[37−50] there is no theoretical reports about the mechanism of platinum-catalyzed cyclopropanation reaction. Thus, in the present study, we have carried out a theoretical investigation at the DFT level of the cyclopropanation reaction catalyzed by Pt complexes, which are expected to provide some helpful information to experimentalists who are interested in this area. Our study intends to resolve the four following problems: (i) which is the nature of the active form of the catalyst, metal-carbene or carbenoid; (ii) what is the mechanistic details of this important reaction (concerted or stepwise reaction pathway and structure of the possible active intermediates); (iii) the effect of the solvent (which is a better solvent, polar or inert); (iv) as compared with catalyst $Cl_2Pd(PH_3)_2$, whether $Cl_2Pt(PH_3)_2$ has the same mechanism as catalyst or not. To these purposes, we have chosen as a model system an ethylene molecule reacting with the active species which forms from a $Cl_2Pt(PH_3)_2$ complex and the $CH_2$ fragment obtained after decomposition of diazomethane.

## Computational Details

The detailed quantum chemical studies on the mechanism of the platinum-catalyzed cyclopropanation reaction with olefin are reported in this paper. The stationary structures of the potential energy surfaces were fully optimized at the B3LYP[51−53] level of theory. Analytical frequency calculations at the same level of theory were performed in order to confirm to the optimized structures to either a minimum or a first-order saddle-point as well as to obtain the zero-point energy correction. Furthermore, intrinsic reaction coordinate (IRC) calculations[54] were performed to confirm that the optimized transition state correctly connects the relevant reactants and products. Geometry optimization for all of the reactants, intermediates, transition states, and products as well as the frequency calculations were carried out with the 6-311G** basis set for the carbon, hydrogen, and chlorine atoms

* Corresponding author. Tel.: +86 931 7970198. E-mail: zhiyuangeng@yahoo.com.cn.

10.1021/jp0732211 CCC: $37.00 
Published on Web 08/31/2007

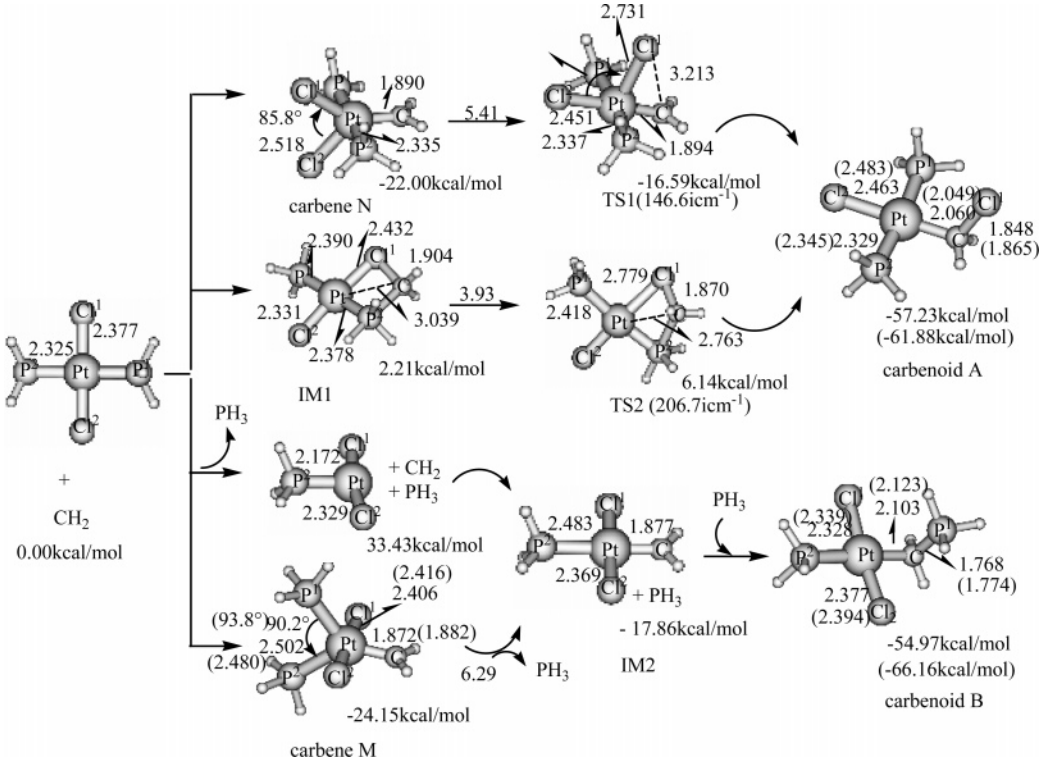


**Figure 1.** Schematic representation of the structures and the formation process of the carbenoids $Cl(PR_3)_2Pt-CH_2Cl$ and $Cl_2(PR_3)Pt-CH_2(PR_3)$ (R = H or $CH_3$) species (bond lengths are in Å and the bond angles in degrees). The relative energy values (kcal/mol) with the ZPE correction of the various species are reported. The data in parentheses represent that the new geometrical parameters while carbene M and carbenoids (A and B) are replaced with the two small $PH_3$ fragments with two ($PMe_3$) ligands.

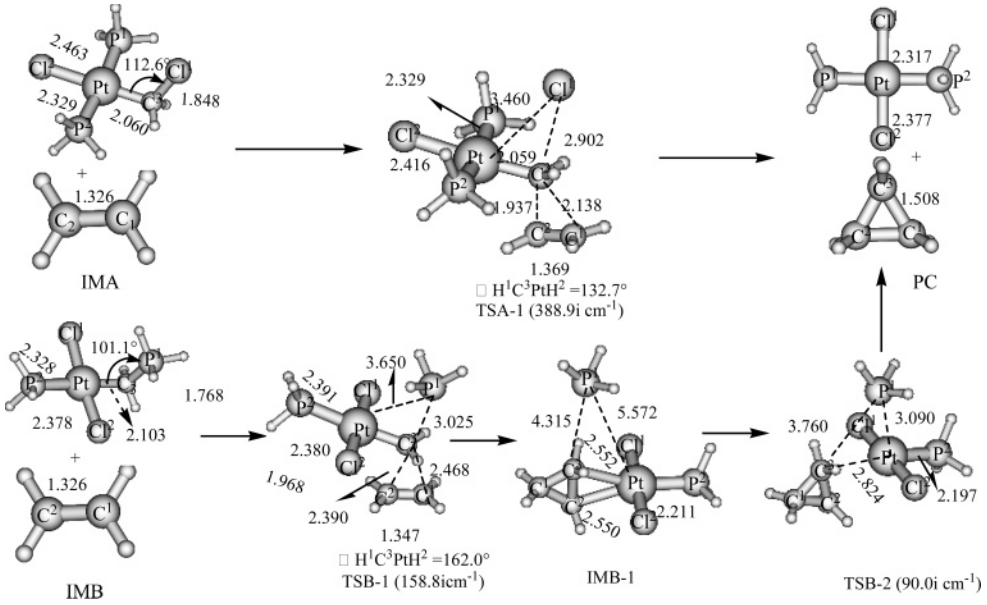


**Figure 2.** Schematic representation of the structures found along path 1: IMA → PC, IMB → PC. Selected key geometry parameters are show for each species with the bond lengths in Å and the bond angles in degrees.

of the reactions investigated.[55] Also, the relativistic core potentials (RECP)[56] were used for the Pt atom. All calculations used the RECP in which 5s, 5p, 5d, and 6s electrons were explicitly treated as "valence" electrons with the remaining electrons replaced by the RECP. Thus, 18 valence electrons RECP were used for the Pt center. In addition, in this RECP, the filled $4f^{14}$ electrons that do not participate actively in the bonding were also included in the core for a total of 60 electrons. The RECP were used in combination with their optimized basis set with an additional f polarization function. In consideration of the solvent effects on the reactions of interest, the polarized continuum model (PCM)[57,58] was applied to the calculations. All of calculations were performed with the Gaussian 98 program.[59]

## Results and Discussion

The optimized stationary structures (minima, saddle points) on the potential energy surfaces of the reactions are depicted schematically in Figures 1−5 with selected key geometry parameters (bond lengths, bond angles, and dihedral angles). The detailed structural parameters and energies for the structures

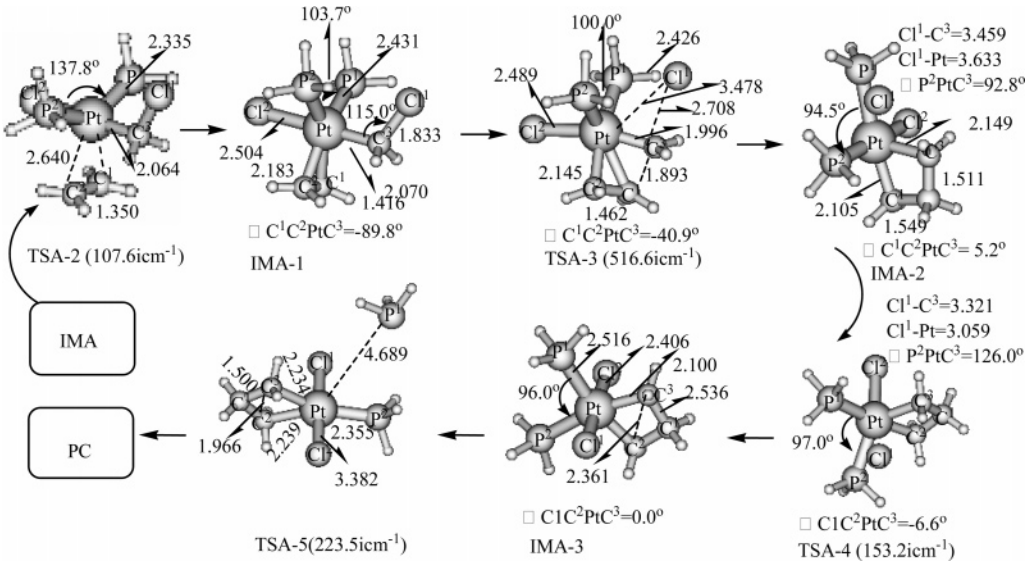


**Figure 3.** Schematic representation of the structures found along path 2 (bond lengths are in Å and angles in degrees) for carbenoid A.

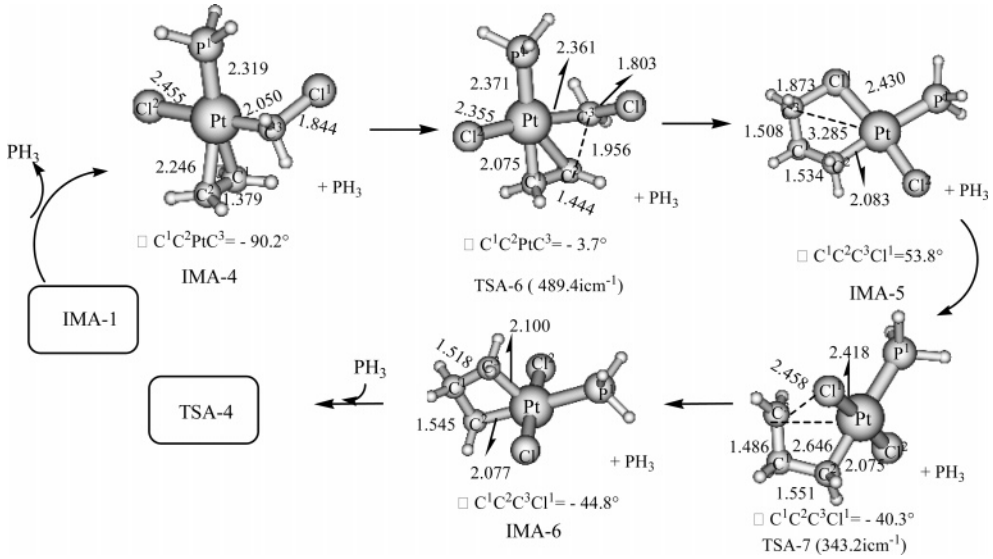


**Figure 4.** Schematic representation of the structures found along path 3.A (bond lengths are in Å and angles in degrees) for $(PH_3)_2Pt(CH_2Cl)$-$Cl+CH_2CH_2$.

determined here are collected in the Supporting Information. The relative energies including zero-point energies (ZPE) are shown graphically in Figure 6 (panels a−d). For the convenience of our discussion in the following sections, some abbreviations are used for different transition states and intermediates, IMA and IMB stand for starting complexes which contain carbenoids (A and B) and ethylene, TS1, TS2, TSA-*n* ($n = 1\sim6$) and TSB-*n* ($n = 1\sim5$) stand for the transition states, IM1, IM2, IMA-*n* ($n = 1\sim6$) and IMB-*n* ($n = 1\sim5$) stand for the intermediates of the reaction process, respectively. PC represents products, $Cl_2Pt(PH_3)_2$ complex and cyclopropane ($C_3H_6$).

**A. Structure of the Active Species.** As described in Figure 1, we have located both the metal-carbenes (M and N) and carbenoids (A and B), which are formed from catalyst $Cl_2Pt(PH_3)_2$ complex and singlet carbene $CH_2$. It has been pointed out that both the singlet carbenoids A and B are more stable than the singlet metal-carbene M by 33.09 and 30.82 kcal/mol, respectively, and the carbene M is also 2.15 kcal/mol lower in energy than carbene N. As shown in Figure 1, 33.43 kcal/mol energy will be required if a $PH_3$ was released from the $Cl_2Pt(PH_3)_2$ complex, but this process only needs 6.29 kcal/mol from carbene M to IM2, and a small energy barrier (5.41 kcal/mol) needs to be overcome from carbine N to TS1. The $CH_2$ can insert into the Pt−Cl bond directly; of course, an intermediate IM1 which is 2.21 kcal/mol higher in energy than $(Cl_2Pt(PH_3)_2 + CH_2)$ has been found in this process. Then a small energy barrier (3.93 kcal/mol) is required to overcome carbenoid A, but we could not find a similar process for the formation of carbenoid B. It is interesting to point out that we could not obtain the transition state for the formation of metal-carbenes (M and N) and the release of $PH_3$. All of these suggest that the platinum atom adopts a four-coordinate structure which has more stability than five-coordinate geometry. We have re-computed the structures of carbene M and carbenoids (A and B) after replacement of the two small $PH_3$ fragments with two ($PMe_3$) ligands (new geometrical parameters in parentheses). A comparison of the three sets of parameters shows that the increase of the steric hindrance has a negligible effect on the molecular geometry. The energy difference between the carbene M and the two carbenoid species (A and B) does not change significantly either, being now 37.74 and 42.01 kcal/mol, respectively. It may be noted that $Cl_2(PMe_3)Pt(CH_2PMe_3)$ is more stable (4.27 kcal/mol) than $Cl(PMe_3)_2Pt(CH_2Cl)$, but this difference does not influence the following discussion. Therefore, carbenoids

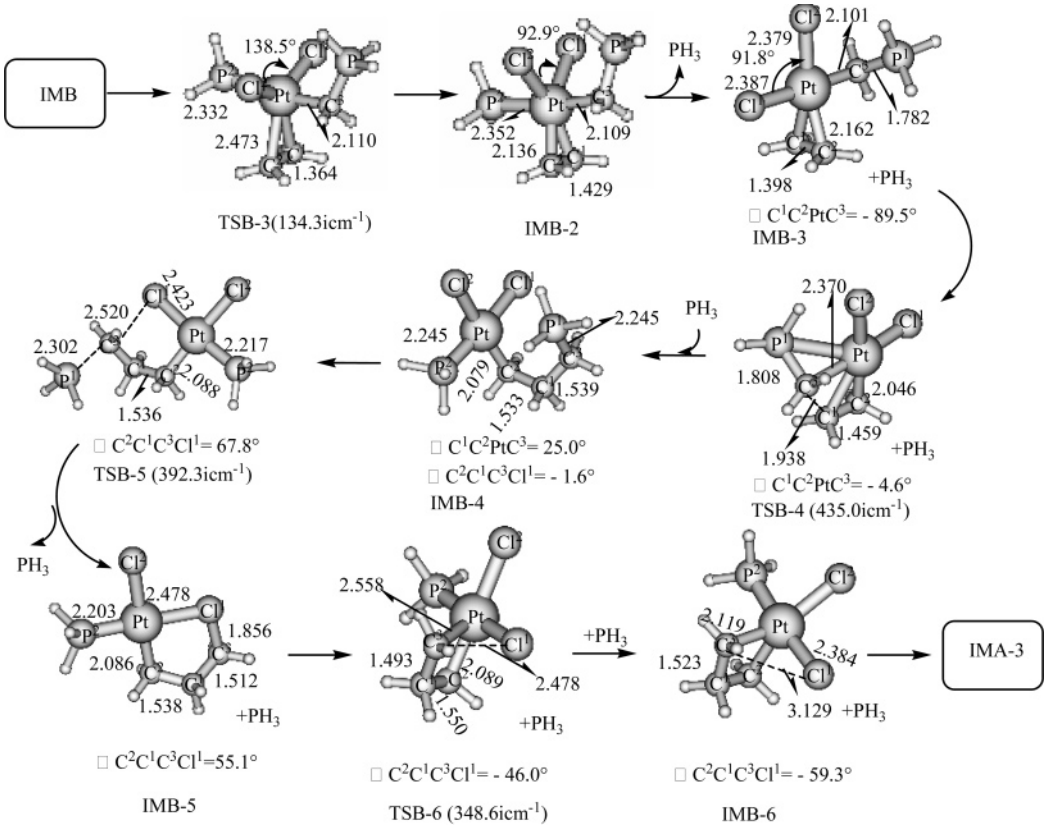


**Figure 5.** Schematic representation of the structures found along path 3.A (bond lengths are in Å and angles in degrees) for $(PH_3)Pt(CH_2PH_3)Cl_2+CH_2$-$CH_2$.

A and B have been selected to study the cyclopropanation reaction. To obtain more reliable data, the solvent (dichloromethane $\epsilon = 8.93$) effect through PCM calculations has been considered at B3LYP/6-311G**/RECP for carbene M and two carbenoids A and B. The results confirm the same trends which indicate that carbenoid A is also more stable than carbenoid B, and the energy difference does not reveal a significant change (only varied from 2.27 kcal/mol to 0.71 kcal/mol). These results indicate that both carbenoids A and B are possible active species for the cyclopropanation reaction. Therefore, all reaction paths that originate from two carbenoids have been carefully investigated. The results are presented and discussed in the following section.

**B. Cyclopropanation Reactions of Carbenoid A and B with Ethylene.** *Path 1. Methylene Transfer Mechanism.* Figure 2 displays the optimized geometry found for the Pt carbenoids A and B, the transition states TSA-1, TSB-1, and TSB-2, and the intermediate IMB-1 for reactions with ethylene through path 1 to produce cyclopropane and $Cl_2Pt(PH_3)_2$. It is a methylene transfer channel which is very similar to that recently found in a theoretical study of the SS cyclopropanation reaction.[36,37] The results show the three-centered transition state TSA-1 where the pseudotrigonal methylene group of the carbenoid adds to the ethylene $\pi$-bond to form two new C−C bonds asynchronously to produce cyclopropane and $Cl_2Pt(PH_3)_2$ for IMA. This is accompanied by a Cl atom migration from carbon to the Pt atom. The distance of $Cl^1-C^3$ changes from 1.848 Å (IMA) to 2.902 Å (TSA-1). The three-centered transition state TSA-1 is similar to that proposed by Molander and co-workers[26,27,60] and Concellón and co-workers[61] to explain the stereochemical features of this type of reaction. However, the cyclopropanation reaction[46] between ethylene and $(PH_3)_2Pd(CH_2Cl)Cl$ would correspond to the loss of a $PH_3$ ligand (the Pd−P distance was 4.342 Å). For the cyclopropanation reaction of IMB, the methylene transfer mechanism needs two steps. The first step corresponds to the formation of an intermediate complex IMB-1 which indicated that the cyclopropane molecule and the $Cl_2Pt(PH_3)_2$ frangment ($C^3-Pt$ bond length is 2.552 Å) are almost completely formed. This is accompanied by weakening of the $P^1-C^3$ bond from 1.768 Å (IMB) to 3.025 Å (TSB-1) and 4.315 Å (IMB-1). However, one $PH_3$ ligand is only weakly interacting with the metal (the $P^1-Pt$ distance is 5.572 Å). Thus, transition state TSB-2 which is described that the $P^1-Pt$ distance further decreases (3.090 Å) and the $C^3-Pt$ distance further increases (2.552 Å) leading to the cyclopropane molecule and a $Cl_2Pt(PH_3)_2$ complex, which enters a new catalytic cycle. Vibrational analysis show that the TSA-1, TSB-1, and TSB-2 have only one imaginary frequency (388.9, 158.8, and 90.0*i* $cm^{-1}$, respectively) and have been confirmed to be the first-order saddle point connecting the corresponding reactants and products by IRC calculations.

Figure 2 shows that the $H^1-C^3-Pt-H^2$ dihedral angle of the TSB-1 is 162.0°, and it indicates the $C^3$ atom is close to a $sp^2$ hybrid structure and is much different from the almost $sp^3$ hybridization structure of $C^3$ atom for the TSA-1 that has a corresponding dihedral angle ($H^1-C^3-Pt-H^2$) of 132.7°. The angles of $Pt-C^3-H^1$ and $H^1-C^3-H^2$ are 121.3° and 116.0° in the TSB-1, respectively, and this is consistent with $C^3$ having noticeable $sp^2$ character with the $Pt-C^3-H^1$ angle increasing from 111.2° expected for an $sp^3$ hybridized carbon. However, compared with carbenoid A, small changes have taken place for the data in TSA-1, which suggest that the $C^3$ atom for TSA-1 remains $sp^3$ hybrid structure. On the other hand, the $C^1-C^2$ distances in TSA-1 and TSB-1 are elongated to 1.369 and 1.347 Å, respectively, from the free ethylene (1.326 Å), and the planar ethylene molecule undergoes a significant pyramidalization of about 19.5 and 5.9° for $C^2$ in the TSA-1 and TSB-1 structures, respectively. It indicates the onset of the $sp^2 \rightarrow sp^3$ rehybrid-

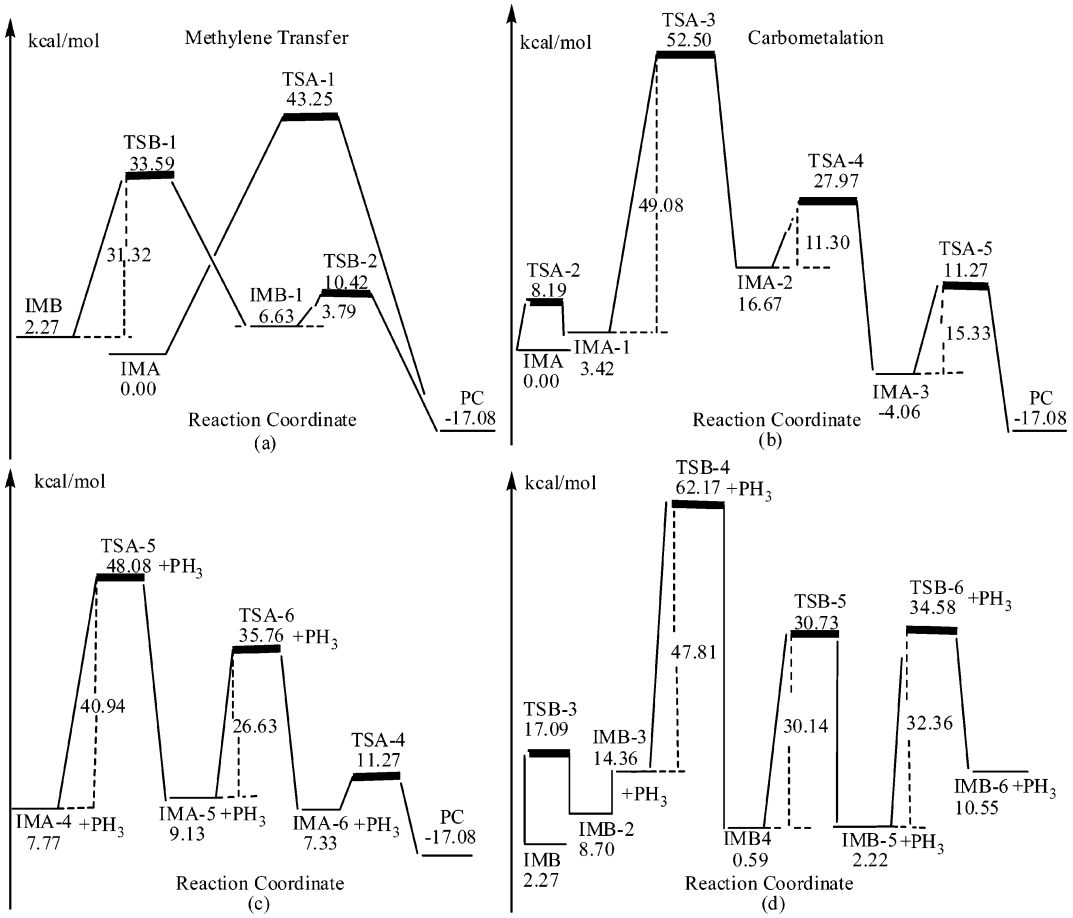


**Figure 6.** Schematic diagram showing the computed relative energy (in kcal/mol) with the ZPE correction for reaction of $(PH_3)_2Pt(CH_2Cl)Cl + CH_2CH_2$ and $(PH_3)Pt(CH_2PH_3)Cl_2 + CH_2CH_2$.

ization required for cyclopropane formation, whereas the pyramidalization is only 0.1 and 2.0° for $C^1$, respectively. This reflects out the asynchronous approach of the $CH_2CH_2$ molecule for the cyclopropanation reaction. As far as the two activation energies ($E_a$) with ZPE correction computed for TSA-1 and TSB-1 are concerned, as presented in Figure 6a, in the former case (carbenoid A), a barrier of 43.25 kcal/mol must be overcome to afford the product (PC, which is 17.08 kcal/mol lower than IMA, and 19.35 kcal/mol more stable than IMB). However, the formation of IMB-1 has a low-energy barrier of 31.27 kcal/mol. From the kinetic point of view, the carbenoid B which leads to cyclopropane is more favored than carbenoid A. Following this, a small barrier of 3.79 kcal/mol should be overcome easily for TSB-2 to product PC.

*Path 2. Carbometalation Mechanism.* As shown in Figure 3, another pathway named the carbometalation process which involves a [2+2] addition of ethylene to the Pt−C bond to form an intermediate (IMA-2) through a four centered transition state (TSA-3) leading to cyclopropane has been found for carbenoid A. In this case, the first step, characterized by an activation barrier of 8.19 kcal/mol, leads to the formation of a preliminary $\pi$ complex IMA-1, where the ethylene molecule weakly interacts with the metal atom. This interaction causes a lengthening of the Pt−P and Pt−Cl bonds with respect to the isolated carbenoid species (from 2.329 to 2.431 and from 2.463 to 2.504 Å, respectively.) A subsequent intramolecular substitution reaction of the intermediate IMA-2 produces the platinumcyclobutane intermediate IMA-3 and the final cyclopropane product. It is interesting to point out that the IMA-3 characterized by $C_{2v}$ symmetry, with the three carbon atom, the metal, and the two $PH_3$ ligands lying in the same plane. Compared with the methylene transfer pathway, relatively large changes are associated with the $C^1-C^2-Pt-C^3$ dihedral angle, $C^3$-$Cl^1$ and Pt−$Cl^1$ distances that vary from −89.8°, 1.833, and 3.295 Å in IMA-1 to −40.9°, +2.708, and +3.478 Å in TSA-2 to 5.2°, 3.459, 3.633 Å in IMA-2. Then the $C^3$-$Cl^1$ is nearly broken and the Pt−$Cl^1$ bond (3.059 Å) is almost formed in TSA-3 which leads to platinumcyclobutane intermediate (Pt−$Cl^1$ bond is 2.406 Å), It must be noted that a reductive elimination step (IMA-3 → PC) needs to leave a $PH_3$ ligand, the Pt−P distance being 4.689 Å. Thus, as given in Figure 6b, more energy is needed to overcome the barrier of the carbometalation pathway from IMA-1 to TSA-3, including the ZPE correction. It is clear that this step is rate-determining in the overall carbometalation process. The similar process has been found for the palladium-catalyzed cyclopropanation reaction, in which the rate-determining step also needs a very high activation energy (about 51.4 kcal/mol). Therefore, according to the results of our computational study, even if the subsequent transformation from the IMA-2 to the products requires two smaller energies (11.30 and 15.33 kcal/mol, respectively), the overall process is unlikely with respect to the energy. For carbenoid B, though a preliminary $\pi$ complex IMB-2 has also been found (as shown in Figure 5), the similar mechanism has not been found, and it is in accordance with the reaction pathway which has been determined for $(PH_3)_2Pd(CH_2Cl)Cl$.[46] Vibrational analysis showed that the TSA-2, TSA-3, TSA-4, and TSA-5 have only one imaginary frequency (107.6, 516.6, 153.2, and 223.5i$cm^{-1}$, respectively).

*Path 3.A. Reaction of a Monophosphinic Species for Carbenois A.* As is clear from Figure 4, apart from methylene transfer and carbometalation mechanisms, the formation of a monophosphinic species is also studied at the same theoretical level. The first step of the process corresponds to the loss of a $PH_3$ ligand and the formation of an intermediate IMA-4 from IMA-1. We also could not obtain the transition state for this process despite detailed investigations of the potential energy surface of Pt−P bond dissociation. The computed energetics suggest that the release of $PH_3$ will easily occur. As shown in Figure 6, after $PH_3$ removal, the energy does not increase significantly (IMA-4 + isolated $PH_3$ is 7.77 kcal/mol higher barrier than IMA). A higher barrier (40.94 kcal/mol) is required to transform IMA-4 to a new intermediate IMA-5 that corresponds to a loose five-membered cycle with a bridged chlorine between the metal and the methylene group. This step can be considered as an insertion reaction of the ethylene molecule into the Pt−C bond. Then a further rearrangement of the intermediate IMA-5 (breaking of the C3−C11 bond and formation of a new Pt−C bond as described by transition state TSA-7 represented in Figure 4) leads, after overcoming a barrier of 26.63 kcal/mol, to the formation of the intermediate IMA-6. It is worth pointing out that the reductive elimination with activation energy of 3.94 kcal/mol leads to the formation of the final complex PC (the $PH_3$ ligand enters again the metal coordination sphere, leading to the transation state TSA-5 which already discussed in path 2). A similar reaction pathway has been determined for $(PH_3)_2Pd(CH_2Cl)Cl$.[46] However, its rate-determining is only required to overcome 29.04 kcal/mol barrier energy at B3LYP/DZVP level. Thus, our calculation results indicate that, as compared with the methylene transfer mechanism, a significantly high barrier makes the process impossible. Vibrational analysis showed that the TSA-6 and TSA-7 have only one imaginary frequency (489.4 and 343.2*i* $cm^{-1}$, respectively).

*Path 3.B. Reaction of a Monophosphinic Species for Carbenoid B.* As displayed in Figure 5, a similar reaction pathway has been determined for carbenoid B. In this case, the formation of the preliminary $\pi$ complex IMB-2 is required to overcome 14.82 kcal/mol from IMB. Then a stronger interaction between ethylene and platinum leads to the formation of a new complex IMB-3, where a phosphine ligand has been expelled from the metal coordination sphere. However, it is pointed out that a transition state for this process has not been found. The energy of the system (as shown in Figure 6d), after $PH_3$ removal, does not increase significantly (IMB-3 + isolated $PH_3$ is 5.66 kcal/mol higher than IMB-2) either. This suggests that the release of $PH_3$ easily occurs. There are three higher barriers, the first associated with transition state TSB-4 (47.81 kcal/mol), the second with transition state TSB-5 (30.14 kcal/mol), and the last with transition state TSB-6 (32.36 kcal/mol), that are required to reach complex IMB-6 which has a cyclic structure (resembling that of IMA-6, Path3-A). It suggests that the reaction pathway remains unlikely on the energy ground.

Three points must be stressed in this process: (i) With the formation of the intermediate IMB-3, a $PH_3$ group will be expeled by the ethylene. However, next arrangement in complex IMB-4 allows $PH_3$ ligand to enter again. (ii) In the step IMB-4 → IMB-5, the chlorine ($Cl^1$) atom forms a new bond with the carbon ($C^3$) to built the cycle and causes the removal of the second $PH_3$ group. Such a complicated structural modification is not found in the transformation IMA-4 →IMA-5, since in IMA-4 the Cl atom is already bonded to the methylene carbon. (iii) The cyclic structure of IMA-5 and IMB-5 can be formed because the chlorine ligand, unlike the $PH_3$ group, after having formed a $\sigma$ bond with one atom (for instance the carbon of the methylene unit), can use one of the lone pairs to interact with another atom (Pt). Thus, a simultaneous interaction with two atomic centers (carbon and platinum atoms) becomes possible. The different nature of the two ligands Cl and $PH_3$ explains why for carbeniod B we have not found a reaction path which is similar to path 2.

**TABLE 1: Schematic Diagram Showing the Effect of Dichloromethane ($\epsilon$ = 8.93), THF ($\epsilon$ = 7.58), and Benzene ($\epsilon$ = 2.25) Solvent on the Cyclopropanation Reactions Investigated Using PCM Method**

| | gas-phase | dichloromethane | THF | benzene |
|---|---|---|---|---|
| IMA → TSA-1 | 43.25 | 25.36 | 25.44 | 33.02 |
| IMB → TSB-1 | 31.32 | 37.62 | 37.42 | 35.35 |
| IMA → 1TSA-3 | 49.08 | 38.53 | 38.97 | 46.28 |
| IMA → 4TSA-5 | 40.94 | 41.84 | 41.81 | 41.58 |
| IMB → 3TSB-4 | 47.81 | 47.18 | 47.20 | 48.77 |

**C. Effect of the Solvent.** Cyclopropanation reactions are usually done in polar organic solvents for a number of carbenoid reagents. For the Pt promoted cyclopropanation reaction, $CH_2Cl_2$ (dielectric constant $\epsilon$ = 8.93) is always used as the solvent. As described in Table 1, we have chosen the rate-determining steps of each reaction channels and studied the changes of activation barrier. It has been found that the results showed some unlike trends and a bigger deviation. For carbenoid A, the activation barrier will be reduced to 25.36 and 38.53 kcal/mol in the paths 1 and 2, respectively. However, the barrier will be able to rise to 38.53 kcal/mol from 31.32 kcal/mol for carbenoid B in path 1. It is difficult to understand why the two barriers do not change significantly with respect to the values in gas-phase in path 3, becoming 41.84 kcal/mol in path 3.A and 47.18 kcal/mol in path 3.B. For clarity, we also study the effect of activation barrier when the dissolvent is THF ($\epsilon$ = 7.58) or benzene ($\epsilon$ = 2.25), and the results show that there is no obvious difference between dichloromethane and THF. However, the effect of inert solvent (benzene) on activation barrier is less obvious than that of dichloromethane and THF. With the aid of Figures 2−5 and Table 1, we also find that one chlorine atom is expelled from carbon ($C^3$) in the step IMA → TSA-1 and IMA-1 → TSA-2, respectively, and one $PH_3$ ligand is released in the step of IMB→TSB-1, but such releases are not found in the steps of IMA-4 → TSA-5 and IMB-3 → TSB-4.These suggest that the effect of solvent is in relation to the release of Cl or $PH_3$ ligands. Specifically, the positive effect of polar solvent is more prominent than inert for the release of Cl ligand, but the negative effect of the polar solvent is a little greater than that for the inert for the release of the $PH_3$ ligand. We also obtain some proofs from the change of the charge. The Mulliken charge indicates that (i) because the $Cl^1$ ligands have significant negative charge (−0.685 in the TSA-1 and −0.619 in the TSA-3) compared with the carbenoid A (−0.146) and IMA-1 (0.131), the other part of two transition states (the geometrical structures have been discussed in paths 1 and 2) except $Cl^1$ atom have more positive charge, which is undoubtedly due to the greater solvation energy of the TSA-1 and TSA-3 in comparison with the carbenoid A and IMA-1; (ii) the $P^1H_3$ ligand has neglectable positive charge (0.008) compared with the carbenoid B (0.548), so the other part of THB-1 has a more positive charge compared with TSA-1 and TSA-3, which made the TSB-1 have smaller solvation energy in comparison with the carbenoid B; (iii) the whole change of the charge is not certainly obvious for the steps of IMA-4 (−0.137, $Cl^1$) to TSA-5 (−0.049, $Cl^1$) and IMB-3 (0.556, $P^1H_3$) to TSB-4(0.560, $P^1H_3$). All of the above-mentioned points indicate that the most favored

reaction channel for cyclopropanation is the methylene transfer path determined for the carbenoid A (path 1) in the presence of the polar solvent (dichloromethane).

## Conclusion

In this paper, we have carried out a theoretical investigation at the DFT (B3LYP) level for the mechanism of the cyclopropanation reaction catalyzed by the $Cl_2Pt(PH_3)_2$ complex. The most important points can be summarized as follows.

(i) The active catalytic species is not a metal-carbene of the type $(PH_3)_2Cl_2Pt{=}CH_2$ whose energy is about 33 kcal/mol higher than the carbenoid complexes $(PH_3)_2Pt(CH_2Cl)Cl$ and $(PH_3)Pt(CH_2PH_3)Cl_2$. The same trend has been proved after replacement of the two small $PH_3$ fragments with two ($PMe_3$) ligands. There is very good agreement with those experimentally determined.[36] So we designate these carbenoid species as "primary" active catalytic species.

(ii) The existence of three different reaction pathways has been demonstrated, which are paths 1 (methylene transfer), 2 (carbometalation for carbenoid A), and 3 (the reaction of a monophosphinic species for carbenoids), respectively. Compared with the catalyst $Cl_2Pd(PH_3)_2$ complex, there are some difference in paths 1 and 3 reaction mechanism. For example, the methylene transfer mechanism for carbenoid A is a concerted pathway, whereas the same process was stepwise for $(PH_3)_2$-$Pd(CH_2Cl)Cl$ in ref 46.

(iii) The most likely reaction channels for cyclopropanation are the two paths determined for the two carbenoid species (path1 and path3-A with a rate-determining barrier of 31.23 and 40.94 kcal/mol, respectively) in the gas phase. The methylene transfer mechanism is a stepwise reaction pathway for carbenoid B, which is not similar to that in the studied theoretical investigations for the zinc,[37] samarium[44] and aluminum[62] carbenoid-promoted cyclopropanation reactions. However, the most likely reaction channel for cyclopropanation of Pd carbenoid $(PH_3)_2Pd(CH_2Cl)Cl$ was a monophosphinic species (the leaving phosphine ligand is only weakly interacting with the metal atom, the Pd−P distance being 4.229 Å) pathway whose rate-determining barrier was about 29.0 kcal/mol.

(iv) The effect of dichloromethane, THF, and benzene solvent on the cyclopropanation reactions is investigated by additional calculations using the PCM method. The barriers are significantly reduced with the increase of the polarity of solvents ($C_6H_{12}$ < THF < $CH_2Cl_2$). Thus dichoromethane was regarded as appropriate solvent, and the activation barrier will be reduced to 25.36 and 38.53 kcal/mol in the methylene transfer path and carbometaiation path for carbenoid A with ethylene, respectively. However, the barrier will be able to rise to 38.53 kcal/mol for carbenoid B with ethylene in the methylene transfer path, but all of these solvents do not affect significantly the activation barriers for monophosphinic species reaction path. Thus, the results show that in solvent the most likely reaction channel is a concerted methylene transfer pathway for carbenoid A.

As mentioned above, compared with the palladium-catalyzed cyclopropanation reaction, the reaction is simpler and the catalysis is more active for the platinum-catalyzed cyclopropanation reaction in the presence of the polar solvent (dichloromethane), and the methylene transfer mechanism is regarded as the most likely reaction channel.

**Supporting Information Available:** Selected output from DFT calculations showing the Cartesian coordinates, Sum of electronic and zero-point energies (au), and vibrational zero-point energies (au) for the reactants, transition states, and products reported in the manuscript are included here. The relativistic core potentials RECP in combination with their optimized basis set with an additional f polarization function were used for Pt in the present studies. The 6-311G** basis set was used for C, P, H, and Cl atoms. This material is available free of charge via the Internet at http://pubs.acs.org.

## References and Notes


(1) Fritschi, H.; Leutenegger, U.; Pfaltz, A. *Angew. Chem., Int Ed. Engl.* **1986**, *25*, 1005.
(2) Doyle, M. P. *Chem. Rev.* **1986**, *86*, 919.
(3) Lautens, M.; Klute, W.; Tam, W. *Chem. Rev.* **1996**, *96*, 49.
(4) Boche, G.; Lohrenz, J. C. W. *Chem. Rev.* **2001**, *101*, 697.
(5) Evans, D. A.; Woerpel, K. A.; Hinman, M. M.; Faul, M. M. *J. Am. Chem. Soc.* **1991**, *113*, 726.
(6) Rodriguez, J. B.; Marquez, V. E.; Nicklaus, M. C.; Barchi, J. J., Jr. *Tetrahedron Lett.* **1993**, *34*, 6233.
(7) Zhao, Y.; Yang, T.-F.; Lee, M.; Chun, B. K.; Du, J.; Schinazi, R. F.; Lee, D.; Newton, M. G.; Chu, C. K. *Tetrahedron Lett.* **1994**, *35*, 5405.
(8) Nishiyama, H.; Itoh, Y.; Matsumoto, H.; Park, S.-B.; Itoh, K. *J. Am. Chem. Soc.* **1994**, *116*, 2223.
(9) Nishiyama, H.; Aoki, K.; Itoh, H.; Iwamura, T.; Sakata, N.; Kurihara, O.; Motoyama, Y. *Chem. Lett.* **1996**, 1071.
(10) Boger, D. L.; Ledeboer, M. W.; Kume, M.; Jin, Q. *Angew. Chem., Int. Ed.* **1999**, *38*, 2424.
(11) Suckling, C. J. *Angew. Chem. Int. Ed. Engl.* **1988**, *27*, 537.
(12) Che, C. M.; Huang, J. S.; Lee, F. W.; Li, Y.; Lai, T. S.; Kwong, H. L.; Teng, P. F.; Lee, W. S.; Lo, W. C.; Peng, S. M.; Zhou, Z. Y. *J. Am. Chem. Soc.* **2001**, *123*, 4119.
(13) Fraile, J. M.; Garcia, J. I.; Martinez-Merino, V.; Mayoral, J. A.; Salvatella, L. *J. Am. Chem. Soc.* **2001**, *123*, 7616.
(14) Rodriguze-Garcia, C.; Oliva, A.; Ortuno, R. M.; Branchhadell, V. *J. Am. Chem. Soc.* **2001**, *123*, 6157.
(15) Straub, B. F.; Hofmann, P. *Angew. Chem, Int. Ed. Engl.* **2001**, *40*, 1288.
(16) Smith, D. A.; Reynolds, D. N.; Woo, L. K. *J. Am. Chem. Soc.* **1993**, *115*, 2511.
(17) Collman, J. P.; Rose, E.; Venburg, G. D. *J. Chem. Soc. Chem. Commun.* **1993**, 934.
(18) Park, S.-B.; Sakata, N.; Nishiyama, H. *Chem. Eur. J.* **1996**, *2*, 303.
(19) Nakamura, E.; Hirai, A.; Nakamura, M. *J. Am. Chem. Soc.* **1998**, *120*, 5844.
(20) Hirai, A.; Nakamura, E.; Nakamura, M. *Chem. Lett.* **1998**, 927.
(21) Jennings, P. W.; Johnson, L. L. *Chem. Rev.* **1994**, *94*, 2241.
(22) Bertani, R.; Biasiolo, M.; Rino, A. *Michelin J. Organomet. Chem.* **2002**, *642*, 32.
(23) Marco-Contelles, J.; Soriano, E. *J. Mol. Struct. (THEOCHEM)* **2006**, *761*, 45.
(24) Dias, E. L.; Nguyen, S. T.; Grubbs, R. H.; Morokuma, K.; Malick, D. K.; Rabuck, A. D.; Raghavachari, K. *J. Am. Chem. Soc.* **1997**, *119*, 3887.
(25) Ulman, M.; Grubbs, R. H. *Organometallics* **1998**, *17*, 2484.
(26) Molander, G. A.; Etter, J. B. *J. Org. Chem.* **1987**, *52*, 3944.
(27) Molander, G. A.; Etter, J. B.; Zinke, P. W. *J. Am. Chem. Soc.* **1987**, *109*, 453.
(28) Grunwald, C.; Gevert, O.; Gonzalez-Herrero, P.; Werner, H. *Organometallics* **1996**, *15*, 1960.
(29) Charette, A. B.; Marcoux, J.-F.; Belanger-Gariepy, F. *J. Am. Chem. Soc.* **1996**, *118*, 6792.
(30) Theberge, C. R.; Verbicky, C. A.; Zercher, C. K. *J. Org. Chem.* **1996**, *61*, 8792.
(31) Nishino, F.; Miki, K.; Kato, Y.; Ohe, K.; Uemura, S. *Org. Lett.* **2003**, *5*, 2615.
(32) Fournier, J.-F.; Mathieu, S.; Charette, A. B. *J. Am. Chem. Soc.* **2005**, *127*, 13140.
(33) Reddy, R. P.; Lee, G. H.; Davies, H. M. L. *Org. Lett.* **2006**, *8*, 3437.
(34) Knorr, R.; Pires, C.; Behringer, C.; Menke, T.; Freudenreich, J.; Rossmann, E. C.; Böhrer, P. *J. Am. Chem. Soc.* **2006**, *128*, 14845.
(35) Simmons, H. E.; Smith, R. D. *J. Am. Chem. Soc.* **1959**, *81*, 4256.
(36) McCrindle, R.; Ferguson, G.; McAlees, A. J.; Arsenault, G. J.; Gupta, A.; Jennings, M. C. *Organometallics* **1995**, *14*, 2741.
(37) Fernando, B.; Andrea, B.; Gian, P. M. *Organometallics* **2000**, *19*, 5529.
(38) Bernardi, F.; Bottoni, A.; Miscione, P. *J. Am. Chem. Soc.* **1997**, *119*, 12300.
(39) Dargel, T. K.; Koch, W. *J. Chem. Soc., Perkin Trans.* **1996**, *2*, 877.

(40) Hermann, H.; Lohrenz, J. C. W.; Kühn, A.; Boche, G. *Tetrahedron* **2000**, *56*, 4109.

(41) Nakamura, E.; Hirai, A.; Nakamura, M. *J. Am. Chem. Soc*. **1998**, *120*, 5844.

(42) Fang, W.-H.; Phillips, D. L.; Wang, D.; Li, Y.-L. *J. Org. Chem*. **2002**, *67*, 154.

(43) Nakamura, M.; Hirai, A.; Nakamura, E. *J. Am. Chem. Soc*. **2003**, *125*, 2341.

(44) Zhao, C. Y.; Wang, D.; Phillips, D. L. *J. Am. Chem. Soc.* **2002**, *124*, 12903.

(45) Zhao, C. Y.; Wang, D.; Phillips, D. L. *J. Am. Chem. Soc*. **2003**, *125*, 15200.

(46) Fernando, B.; Andrea, B.; Gian, P. M. *Organometallics* **2001**, *20*, 2751.

(47) Julian, R. R.; May, J. A.; Stoltz, B. M.; Beauchamp, J. L. *J. Am. Chem. Soc.* **2003**, *125*, 4478.

(48) Fernando, B.; Andrea, B.; Gian, P. M. *J. Am. Chem. Soc*. **1997**, *119*, 12300.

(49) Fraile, J. M.; García, J. I.; Martínez-Merino, V. *J. Am. Chem. Soc*. **2001**, *123*, 7616.

(50) Wang, D.; Phillips, D. L.; Fang, W. H. *Organometallics* **2002**, *21*, 5901.

(51) Becke, A. D. *J. Chem. Phys.* **1993**, *98*, 5648.

(52) Becke, A. D. *Phys. Rev. A* **1988**, *38*, 3098.

(53) Lee, C.; Yang, W.; Parr, R. G. *Phys. Rev. B* **1988**, *37*, 785.

(54) Gonzalez, C.; Schlegel, H. B. *J. Chem. Phys*. **1989**, *90*, 2154; *J. Phys. Chem*. **1990**, *94*, 5523.

(55) Glukhovtse, M. N.; Pross, A.; McGrath, M. P.; Radom, L. *J. Chem. Phys.* **1995**, *103*, 1878.

(56) Andrae, D.; Haeussermann, U.; Dolg, M.; Stoll, H.; Theor, H. P. *Chim. Acta*. **1990**, *77*, 123.

(57) Miertus, S.; Scrocco, E.; Tomasi, J. *J. Chem. Phys*. **1981**, *55*, 117.

(58) Miertus, S.; Tomasi, J. *J. Chem. Phys.* **1982**, *65*, 239.

(59) Frisch, M. J.; Trucks, G. W.; Schlegel, H. B.; Scuseria, G. E.; Robb, M. A.; Cheeseman, J. R.; Zakrzewski, V. G.; Montgomery, J. A., Jr.; Stratmann, R. E.; Burant, J. C.; Dapprich, S.; Millam, J. M.; Daniels, A. D.; Kudin, K. N.; Strain, M. C.; Farkas, O.; Tomasi, J.; Barone, V.; Cossi, M.; Cammi, R.; Mennucci, B.; Pomelli, C.; Adamo, C.; Clifford, S.; Ochterski, J.; Petersson, G. A.; Ayala, P. Y.; Cui, Q.; Morokuma, K.; Malick, D. K.; Rabuck, A. D.; Raghavachari, K.; Foresman, J. B.; Cioslowski, J.; Ortiz, J. V.; Stefanov, B. B.; Liu, G.; Liashenko, A.; Piskorz, P.; Komaromi, I.; Gomperts, R.; Martin, R. L.; Fox, D. J.; Keith, T.; Al-Laham, M. A.; Peng, C. Y.; Nanayakkara, A.; Gonzalez, C.; Challacombe, M.; Gill, P. M. W.; Johnson, B. G.; Chen, W.; Wong, M. W.; Andres, J. L.; Head-Gordon, M.; Replogle, E. S.; Pople, J. A. *Gaussian 98*, revision A.5; Gaussian, Inc.: Pittsburgh, PA, 1998.

(60) Molander, G. A.; Harring, L. S. *J. Org. Chem*. **1989**, *54*, 3525.

(61) Concello′n, J. M.; Rodr′guez-Solla, H.; Go′mez, C. *Angew. Chem., Int. Ed.* **2002**, *41*, 1917.

(62) Li, Z. H.; Ke, Z. F.; Zhao, C. Y.; Geng, Z. Y.; Phillips, D. L. *Organometallics* **2006**, *25*, 3735.